HHS Public Access

Author manuscript

Nat Genet. Author manuscript; available in PMC 2017 August 31.

Published in final edited form as:

Nat Genet. 2007 October ; 39(10): 1225–1234. doi:10.1038/ng2112.

Modulation of morphogenesis by noncanonical Wnt signaling requires ATF/CREB family–mediated transcriptional activation of TGFβ2

Wenlai Zhou[1,9], **Lizhu Lin**[2,9], **Arindam Majumdar**[3], **Xue Li**[1], **Xiaoxue Zhang**[2], **Wei Liu**[4], **Leah Etheridge**[5], **Yunqing Shi**[2], **James Martin**[4], **Wim Van de Ven**[6], **Vesa Kaartinen**[7], **Anthony Wynshaw-Boris**[5], **Andrew P McMahon**[8], **Michael G Rosenfeld**[1], and **Sylvia M Evans**[2]

[1]Howard Hughes Medical Institute and Department of Medicine, University of California, San Diego, La Jolla, California 92093, USA

[2]Skaggs School of Pharmacy, Departments of Pharmacology and Medicine, University of California, San Diego, La Jolla, California 92093, USA

[3]Division of Matrix Biology, Department of Medical Biochemistry and Biophysics, Karolinska Institute, Scheeles väg2, Plan 4 B1, SE-171 77 Stockholm, Sweden

[4]Alkek Institute of Biosciences and Technology, Texas A&M System Health Science Center, Houston, Texas 77030, USA

[5]Department of Pediatrics, the Comprehensive Cancer Center, University of California, San Diego, La Jolla, California 92093, USA

[6]Laboratory for Molecular Oncology, Department of Human Genetics, University of Leuven, B-3000, Belgium

[7]Department of Pathology, Keck School of Medicine, University of Southern California, Los Angeles, California 90033, USA

[8]Department of Molecular and Cellular Biology, Harvard University, Cambridge, Massachusetts 02138, USA

Abstract

Transcriptional readout downstream of canonical Wnt signaling is known to be mediated by β-catenin activation of well-described targets, but potential transcriptional readout in response to noncanonical Wnt signaling remains poorly understood. Here, we define a transcriptional pathway important in noncanonical Wnt signaling. We have found that *Wnt11* is a direct target of a canonical β-catenin pathway in developing heart and that *Wnt11* mutants show cardiac outflow tract defects. We provide genetic and biochemical evidence that Wnt11 signaling affects

Correspondence should be addressed to S.M.E. (syevans@ucsd.edu) or M.G.R. (mrosenfeld@ucsd.edu).

[9]These authors contributed equally to this work.

Note: Supplementary information is available on the Nature Genetics website.

AUTHOR CONTRIBUTIONS

W.Z. and L.L. contributed equally to this work, and their names are interchangeable in this paper.

extracellular matrix composition, cytoskeletal rearrangements and polarized cell movement required for morphogenesis of the cardiac outflow tract. Notably, transforming growth factor β2 (TGFβ2), a key effector of organ morphogenesis, is regulated by Wnt11-mediated noncanonical signaling in developing heart and somites via one or more activating transcription factor (ATF)/cyclic AMP response element binding protein (CREB) family members. Thus, we propose that transcriptional readout mediated at least in part by a Wnt11→ATF/CREB→TGFβ2 pathway is critical in regulating morphogenesis in response to noncanonical Wnt signaling.

Morphogenesis involves hierarchical integration of signaling pathways and transcription factor networks that coordinately regulate cell polarity, adhesion and migration events. Noncanonical Wnt pathways are important in polarized cell movement and organ morphogenesis through activation of cytoskeletal pathways, such those involving as the small GTPases rhoA and cdc42, rho kinase, protein kinase C (PKC) and Jun N-terminal kinase (JNK)[1], and are involved in cardiac outflow tract remodeling and morphogenesis. Mice with mutations in one of the cell polarity genes, *Vangl2* (Van Gogh-like 2), also known as *Ltap* (looptail-associated protein), show cardiac outflow tract defects[2,3]. However, potential transcriptional targets of noncanonical Wnt pathways required for morphogenesis have not been defined[4].

Outflow tract formation[5,6] involves interactions between diverse cell types in the region of the pharyngeal splanchnic mesenchyme, the anterior or secondary heart field that gives rise to the myocardium of the outflow tract of the heart and its endothelial lining[7]. Remodeling of the outflow region of the heart results in concordant connections from the left ventricle to the aorta and the systemic circulation and from the right ventricle to the pulmonary trunk and the pulmonary circulation. Congenital defects involving the outflow tract include transposition of the great arteries (TGA), double outlet right ventricle (DORV) and persistent truncus arteriosus (PTA), where a single outflow tract vessel is observed in place of the normal aorta and pulmonary artery. Several mouse mutants have been reported that have cardiac outflow tract defects modeling those seen in humans with congenital heart disease[8].

Here, we identify Wnt11 as the noncanonical Wnt implicated in outflow tract morphogenesis, and we show that activation of transcription of *Tgfb2* (encoding TGFβ2) mediated by ATF family transcription factors is a key effector of noncanonical Wnt signaling. We demonstrate that this pathway operates during heart and somite development in mammals, suggesting its general significance. Our results also highlight a requirement for Wnt11 in the integration and crosstalk between three major signaling pathways—the canonical Wnt pathway, the noncanonical Wnt pathway and TGFβ signaling—to achieve correct cardiac outflow tract morphogenesis.

RESULTS

Wnt11 is a downstream target of Pitx2 and β-catenin

Mice that are null for *Pitx2*, encoding a bicoid-like homeodomain protein implicated in Rieger's syndrome type I[9], show DORV, TGA or PTA[10]. During outflow tract formation,

Pitx2 is a downstream target of a canonical Wnt-Dishevelled pathway[10], presenting a model to study integration of signaling pathways during tissue morphogenesis. To study downstream targets of Pitx2, we performed an RNA profiling analysis by comparing RNA from control C2C12 cells and from C2C12 cells treated with short hairpin RNA (shRNA) targeting *Pitx2* mRNA. Real-time RT-PCR analysis indicated that *Pitx2* transcripts were substantially downregulated by shRNA against *Pitx2* mRNA (Fig. 1a), and Pitx2 protein expression was also significantly downregulated by shRNA against *Pitx2* (Supplementary Fig. 1 online). Knockdown of endogenous *Pitx2* expression uncovered a number of genes that were potentially regulated by Pitx2, indirectly or directly (data not shown). One target gene selected for further study was that encoding the secreted glycoprotein growth factor Wnt11. *Wnt11* transcripts were decreased by more than 50% in C2C12 cells treated with shRNA targeted to *Pitx2* mRNA (Fig. 1a).

We performed chromatin immunoprecipitation (ChIP) assays using specific antibodies against Pitx2, which showed that Pitx2 is present on the *Wnt11* promoter in a region containing a perfect consensus Pitx2 response element within the 5′ regulatory region[11] (Fig. 1b) in proliferating C2C12 cells. Expression of a reporter gene under the control of a 2-kb fragment of the *Wnt11* promoter was substantially higher in a transient transfection assay by cotransfection with expression vectors encoding different *Pitx2* isoforms in C2C12 cells (Fig. 1c). In contrast, neither Pitx2a nor Pitx2c activated expression of the *Wnt11* 2-kb promoter reporter containing mutated Pitx2 binding sites, further supporting the direct requirement for Pitx2 in the activation of *Wnt11* transcription (Fig. 1c). We confirmed the biological significance of these data by examining *Pitx2* mutant mice by real-time RT-PCR (Supplementary Fig. 2 online), as well as by *in situ* hybridization (Fig. 1d), which showed that *Wnt11* expression was downregulated in pharyngeal splanchnic mesoderm of the secondary heart field and in the outflow tract where *Pitx2* and *Wnt11* are coexpressed[12–14].

Because β-catenin is a coactivator for Pitx2-mediated induction of expression of *Ccnd2* (encoding cyclin D2)[10] and has been shown to be upstream of *Wnt11 in vivo*[15], we examined whether β-catenin was directly required in concert with Pitx2 for *Wnt11* expression. *Wnt11* transcripts were rapidly (within 30–60 min) and robustly induced upon treatment with lithium chloride in C2C12 cells (Fig. 1e). Expression of a 2-kb *Wnt11* promoter-luciferase construct was activated by either lithium chloride or Wnt3a ligand treatment, and this induction was abolished by addition of short interfering RNA (siRNA) against either *Pitx2* or *Ctnnb1* (encoding β-catenin) (Fig. 1f). However, the *Wnt11* promoter with a mutated Pitx2 binding site was not activated in response to either lithium chloride or Wnt3a ligand treatment (Fig. 1f). Using ChIP analysis in C2C12 cells, we found very little, if any, Pitx2 present on the *Wnt11* promoter in cells maintained in the absence of lithium chloride and serum, whereas addition of lithium chloride caused a marked recruitment of Pitx2 and β-catenin to the *Wnt11* promoter, and the corepressor HDAC1 was dismissed (Fig. 1g). These findings show that activation of *Wnt11* by canonical Wnt signaling is dependent on recruitment of Pitx2 and β-catenin to the *Wnt11* promoter. To confirm recruitment of Pitx2 and β-catenin to the *Wnt11* promoter *in vivo* in the developing heart, ChIP analysis was performed using heart tissue dissected from E9.5 mouse embryos, demonstrating that both Pitx2 and β-catenin were specifically recruited to the 5′ promoter region of the *Wnt11* gene (Fig. 1h). We have also observed specific downregulation of *Wnt11* in a cardiac-

specific knockout of β-catenin[15]. Consistent with this, dermomyotomal expression of Wnt11 in both chick and mouse requires canonical Wnt signaling[16–18], and studies in chick embryos have shown that perturbation of *Wnt11* expression is correlated with abnormal myotome formation[16]. These results indicate that Pitx2 and the Wnt/β-catenin pathway function in concert to activate the *Wnt11* promoter.

Cardiac phenotype in *Wnt11*$^{-/-}$ mutants

To determine whether Wnt11 is a critical downstream effector of Pitx2 during morphogenesis, we examined the cardiac phenotype of *Wnt11* mutants[19], and we found that *Wnt11* mutants, like *Pitx2* mutants, showed conotruncal defects. At E9.5, outflow tracts of *Wnt11* mutants were shorter than those of wild-type littermates (Fig. 2a,b). At E11.5, mutant outflow tracts were still shorter and emanated straight down from the pharyngeal region, lacking the rightward curve that was evident in wild-type embryos (Fig. 2c,d). In wild-type embryos at E12.5, the outflow tract has been partitioned into the aorta and pulmonary artery; the aorta arises from the left ventricle and the pulmonary artery from the right ventricle (Fig. 2e,g). In contrast, in *Wnt11* mutants, both vessels were connected to the right ventricle, resulting in DORV (Fig. 2f,h). Plastic dye injections (Fig. 2i,j) or whole-mount (Fig. 2k,l) and section analyses (Fig. 2m–p) of neonatal hearts from *Wnt11* mutants and wild-type littermates demonstrated that TGA or, more infrequently, PTA had occurred in *Wnt11* mutants. Penetrance of the outflow tract phenotype was 100%. Outflow tract defects were accompanied by ventricular septal defects (VSD) (Fig. 2p). *Wnt11* mutants also showed aortic arch artery defects, as visualized by ink injection (Fig. 2q–t and Supplementary Fig. 3a,*b* online).

As outflow tract defects can be indicative of aberrant cardiac neural crest migration, we investigated whether cardiac neural crest cell migration into the outflow tract occurred in *Wnt11* mutants using *Wnt1-Cre;R26R* lineage analysis[20] in wild-type and *Wnt11* mutant backgrounds. Results of this analysis showed that cardiac neural crest cell migration still occurred in *Wnt11* mutants (Fig. 2u–x), and whole-mount *in situ* hybridization with markers of cardiac neural crest yielded similar results (data not shown). As the outflow tract is derived from the secondary heart field, which is marked by expression of Islet1 (*Isl1*)[21], we also investigated the fate of secondary heart field descendents by *Isl1-Cre;R26R* lineage analysis in wild-type and *Wnt11* mutant backgrounds. Secondary heart field lineages were present in *Wnt11* mutants (Supplementary Fig. 3c–f online).

Tgfb2 is downregulated in *Wnt11*$^{-/-}$ mutants

To define potential effector targets downstream of Wnt11 required for cardiac morphogenesis, we performed whole-mount RNA *in situ* analysis with probes for a number of genes that, when mutated, give rise to cardiac phenotypes similar to those observed in *Wnt11*-and *Pitx2*-null mice[8]. Expression of *Fgf8*, *Tbx1*, *Pitx2*, *Notch1*, *Bmp4* and *Edn1* was unaffected in *Wnt11* mutants (data not shown). In contrast, expression of *Tgfb2* was downregulated by E9.5 in *Wnt11* mutants in pharyngeal splanchnic mesoderm of the secondary heart field and in the outflow tract, the dermomyotome of the somite, the head and the posterior regions[14,22]. *Tgfb2* and *Wnt11* are coexpressed in each of these regions[14,22] (Fig. 3a–h). *Tgfb2* was also downregulated in *Wnt11* E9.5 mutant hearts by

real-time RT-PCR analysis (Supplementary Fig. 4a online). Mice null for *Tgfb2* show TGA, ventricular septal defects, defective myocardialization of the outflow tract and anomalous apoptosis within the cushions, supporting a causal role for downregulation of *Tgfb2* in the *Wnt11*$^{-/-}$ cardiac phenotype[23]. *Tgfb2* was similarly downregulated in *Pitx2* mutants, as shown by *in situ* hybridization and real-time PCR analysis (Fig. 3i–l and Supplementary Fig. 4b online). Looptail mice have outflow tract defects consequent to mutation of *Vangl2*, encoding a homolog of *Drosophila melanogaster* Van Gogh (also called Strabismus). Van Gogh is a component of a noncanonical Wnt planar cell polarity pathway in *D. melanogaster*, and Vangl2 has recently been shown to be a component in a planar cell polarity pathway in vertebrates[24]. These observations suggested that TGFβ2 might also function downstream of *Vangl2* in outflow tract morphogenesis. To investigate this possibility, we examined expression of *Tgfb2* in Looptail mutants and found that its expression was downregulated in pharyngeal mesoderm, outflow tract and somites by *in situ* hybridization or real-time PCR analysis, as seen for *Wnt11* mutants, supporting a common genetic pathway (Fig. 3m,n and Supplementary Fig. 4c online). Ablation of *Hspg2* (encoding perlecan) results in TGA[25]. Transcriptional studies have shown that the *Hspg2* promoter is activated in response to TGFβ signaling[26]. We also observed specific downregulation of *Hspg2* in the outflow tract of *Wnt11* mutants (Fig. 3o,p).

Tgfb2 is regulated by a Wnt11→JNK→ATF/CREB pathway

Consistent with our *in vivo* observation that *Tgfb2* was downregulated in *Wnt11* mutants in both outflow tract and somitic mesoderm, treatment of C2C12 cells with Wnt11-conditioned medium[27] resulted in a rapid (60 min) and more than 2.5-fold induction of *Tgfb2* transcripts, as shown by real-time RT-PCR analysis (Fig. 4a). As JNK pathways are downstream of Wnt11 in other contexts, we examined the dependence of *Tgfb2* induction on JNK signaling. Induction of *Tgfb2* by Wnt11 was abolished by addition of SP600125, an anthra-pyrazolone inhibitor of JNK[28] (Fig. 4a). We observed phosphorylation and activation of JNK in response to Wnt11 treatment of C2C12 cells, as shown by increased phosphorylation of ATF2 and c-Jun (Fig. 4b). To investigate the possible involvement of the canonical pathway, we assessed levels of β-catenin protein in response to stimulation with Wnt11 conditioned medium. Because β-catenin is stabilized in response to canonical Wnt signaling, but we did not observe an increase in β-catenin protein in response to Wnt11 stimulation of C2C12 cells (Fig. 4b); Wnt11 did not seem to function as a canonical Wnt signal. Activity of Wnt11 in conditioned medium was confirmed by its ability to counteract β-catenin–mediated activation of a TopFlash reporter[29] in C2C12 cells (Supplementary Fig. 5 online). Thus, Wnt11 signaling upregulates *Tgfb2* through a noncanonical Wnt signaling pathway involving JNK activation.

The *Tgfb2* promoter contains several evolutionarily conserved elements, including an ATF2 site, and is activated by ATF2, JNK and p38 (refs. 30,31). ATF2 binds to CREs and stimulates CRE-dependent transcription[32]. ATF2 is a histone acetyltransferase (HAT) that specifically acetylates histones H2B and H4. Phosphorylation of ATF2 controls its HAT activity and its action on CRE-dependent transcription[33]. ATF2 is also a downstream target of TGFβ-activated kinase 1 (TAK1) and p38 kinases, which are downstream of bone morphogenetic protein (BMP) signaling[34]. A number of studies have shown a key role for

BMP signaling in cardiac outflow tract morphogenesis[35,36]. To examine the action of ATF2 on the *Tgfb2* promoter in response to Wnt11 stimulation, we transfected a construct containing a *Tgfb2* promoter (bases −77 to +63) driving a luciferase reporter into C2C12 cells treated with either control medium or Wnt11-conditioned medium. Wnt11-conditioned medium activated the *Tgfb2* promoter-luciferase reporter but not its counterpart containing a mutation of the conserved ATF2 binding site (Fig. 4c). Induction of the *Tgfb2* promoter-reporter was abolished by addition of siRNA against *ATF2* but was unaffected by the addition of siRNA to *Ctnnb1* (encoding β-catenin) (Fig. 4c), which further supports the conclusion that β-catenin is not required for the induction of *Tgfb2* promoter activity by Wnt11.

In vitro and *in vivo* ChIP analyses were consistent with these findings. The phosphorylated form of ATF2, as well as acetylated histone H4, were specifically recruited onto the *Tgfb2* promoter after stimulation of C2C12 cells with Wnt11-conditioned medium (Fig. 4d). In contrast, neither the phosphorylated form of c-Jun nor β-catenin was recruited to the *Tgfb2* promoter (Fig. 4d). ChIP analysis using embryonic heart tissue from E9.5 embryos gave similar results, showing binding of phosphorylated ATF2 and acetylated histone H4 to the *Tgfb2* promoter *in vivo* (Fig. 4e). Neither β-catenin nor Pitx2 bound the *Tgfb2* promoter (Fig. 4e). In contrast, both β-catenin and Pitx2, but not phosphorylated ATF2, bound to the *Wnt11* promoter *in vivo* (Fig. 4e). To investigate perturbation of this pathway in *Wnt11* mutants, we performed ChIP analysis on E9.5 embryonic heart extracts from *Wnt11* mutants and control littermates. This analysis showed a loss of binding of phosphorylated ATF2 to the *Tgfb2* promoter in *Wnt11* mutants (Fig. 4f). Together, these data indicate that phosphorylation of ATF2 downstream of noncanonical signaling by Wnt11 is required to activate transcription of TGFβ2, a key regulator of morphogenesis.

As Wnt11 activation of *Tgfb2* occurred via a conserved ATF2 element, we tested whether *Tgfb2* expression in the embryo could also be controlled by a Wnt11→ATF2 signaling pathway. Selecting potential *Tgfb2* control regions that showed a high degree of evolutionary conservation, including three ATF2 sites, we generated transgenic embryos with a 3.2-kb *Tgfb2* promoter fragment and a 1.2-kb 5′ UTR sequence placed upstream of a lacZ reporter gene, followed by the first 6.3 kb of intron 1. We obtained a total of nine independently generated transgenic embryos that were positive for the transgene, and, of these, four showed a consistent expression pattern that recapitulated the early expression of *Tgfb2* in the secondary heart field and its derivatives, including the cardiac outflow tract and right ventricle, and also in the somites (Fig. 4g). We also generated transgenic embryos using the same construct containing mutations in each of the three conserved ATF2 elements found within this promoter fragment of the *Tgfb2* gene. None of the eight independently generated transgenic embryos that were positive for the transgene showed any lacZ expression (Fig. 4g). Thus, Wnt11-regulated ATF2 sites within the *Tgfb2* promoter targeted somite and secondary heart field expression in transgenic mice.

ATF2 mutant mice show chondrodysplasia, neurological defects and features of severe respiratory distress[37,38]. We did not observe a cardiac phenotype in ATF2 mutant mice (data not shown). However, there are several highly related genes in the ATF2 family that have been shown to activate genes in a functionally redundant manner *in vitro* and *in vivo*[39,40]. To

further examine the requirement for the ATF/CREB family in TGFβ2 expression and cardiac morphogenesis, we generated transgenic embryos that were positive for a dominant-negative ATF2 transgene. Of four independently generated embryos containing this transgene, two showed shortened cardiac outflow tract phenotypes similar to those observed in *Wnt11* or *Tgfb2* mutants (Fig. 4h). To examine whether expression of the dominant-negative ATF2 resulted in decreased expression of *Tgfb2*, we performed RNA *in situ* hybridization on these embryos and found that *Tgfb2* expression was selectively decreased in the secondary heart field within the heart and in the somites of the two embryos that showed outflow tract defects (Fig. 4h). These data demonstrate an *in vivo* requirement for ATF2 and related transcription factors in outflow tract morphogenesis and in the regulation of *TGFβ2* expression within developing heart and somites.

Perturbations of cytoarchitecture in *Wnt11* mutants

Because morphogenetic movements mediated by the noncanonical pathway require ordered cytoarchitectural alterations both within cells and between cells, we performed histochemical staining on sections from *Wnt11* mutants and wild-type littermate controls to examine cytoskeletal structure (phalloidin staining for cytoskeletal actin) (Fig. 5 and Supplementary Fig. 6a,b online) and immunostaining for markers for appropriately localized basal lamina (laminin α-5) (Fig. 5e,f), or for apical/basal polarity (integrin β1) (Fig. 5i,j). Myocardial cells of the distal outflow tract in *Wnt11* mutants showed perturbations in each of these aspects of cytoarchitecture relative to control littermates. Consistent with TGFβ2 being a downstream effector in this pathway, basal localization of laminin α-5 was also perturbed in *Tgfb2* mutants (Fig. 5g,h). Staining for the adherens junction marker N-cadherin uncovered a lack of organized epithelial structure in outflow tract myocardium of *Wnt11* mutants, compared with that of control littermates (Supplementary Fig. 6c,d online). These observations suggest that aberrant myocardial cell cytoarchitecture in outflow tracts of *Wnt11* mutants may be consequent to decreased TGFβ2 in splanchnic mesoderm of the secondary heart field and the outflow tract that derives from it.

Staining of sections with antibody against myosin heavy chain (MF20) to examine myocardial cell structure at E12.5 also showed additional cytoarchitectural alterations in *Wnt11* mutant outflow tract compared with the corresponding cells in wild-type littermate controls (Supplementary Fig. 6e,f online). At this stage, myocardial cells of the outflow tract also express α-smooth muscle actin, and staining for expression of α-smooth muscle actin gave comparable results as for MF20 (Fig. 5k,l). In wild-type sections at E12.5, myocardial cells adjacent to mesenchymal cells lose their epithelial character and show stress fibers elongating toward the mesenchymal cell layer, whereas in *Wnt11* mutant sections, comparable myocardial cells appeared more rounded. These changes in cytoarchitecture are a prelude to the myocardialization of the outflow tract septum that will occur at later stages[41], and a similar phenotype has been observed in Looptail mutants[3]. Scribble[42], which functions with Vangl2 in cell polarity pathways, is expressed at E11.5 in an ordered perimembranous distribution in myocardial cells, and is observed at high levels in a few cells within the mesenchyme adjacent to the myocardium (Fig. 5m). In *Wnt11* mutants, Scribble expression was severely reduced within myocardium and was not present in adjacent mesenchyme (Fig. 5n). These defects in *Wnt11* and Looptail mutants are probably

(at least in part) consequent to the observed downregulation of TGFβ2, as we observed similar defects in cytoarchitecture in *Tgfb2* mutant mice, and previous experiments have demonstrated defects in myocardialization in *Tgfb2* mutants[23].

Because *Pitx2*, *Wnt11* and *Tgfb2* are expressed not only in myocardium but also in endothelial cells of the outflow tract, we also investigated the cytoarchitecture of endothelial cells by examining expression of vascular endothelial cadherin and PECAM by immunostaining (Fig. 6a–f). Our results demonstrated that tight adhesion between juxtaposed endothelial layers, which ultimately provides tissue continuity within the spiral septum of the outflow tract in wild-type embryos, was disrupted in *Wnt11* mutants. At E14.5 in wild-type embryos, myocardialization of the forming septum of the proximal outflow tract was evidenced by expression of smooth muscle actin (Fig. 6g). In *Wnt11* mutants, there was no expression of smooth muscle actin in this region (Fig. 6h), demonstrating a lack of muscularization of the septum, which may be a secondary outcome consequent to loss of Wnt11. By E14.5, the aorta and pulmonary artery are surrounded by smooth muscle cells derived largely from neural crest. We observed expression of smooth muscle actin in this region in both wild-type and *Wnt11* mutant mice (Fig. 6g,h). Changes in cellular architecture can affect proliferation or apoptosis. We examined proliferation in *Wnt11* mutant and wild-type embryos from E8.5 to E14.5 by antibody staining to phosphorylated histone H3 and did not find any differences in proliferation rate in myocardium or endocardium between mutant and control litter-mates (data not shown). Examination of apoptosis by antibody staining to cleaved caspase 3 at E10.5 and E14.5 did not uncover any changes at E10.5 but demonstrated increased apoptosis at E14.5 in cushion mesenchyme of *Wnt11* mutant embryos relative to wild-type controls (Supplementary Fig. 7a–d online). Again, these findings are consistent with previous observations in *Tgfb2* mutants[23].

DISCUSSION

We have identified Wnt11 as the noncanonical Wnt implicated in outflow tract morphogenesis and have found that activation of *Tgfb2* transcription mediated by ATF/CREB is regulated by noncanonical Wnt signaling. This pathway operates in both heart and somite development in mammals, suggesting the general significance of the pathway we have defined. We have also provided evidence that disruption of outflow tract morphology observed in Wnt11-deficient embryos is associated with a number of specific changes in cytoarchitecture of the myocardial wall, the endocardium of the outflow tract and the cardiac outflow tract cushions, as well as with lack of myocardialization of the outflow tract septum. Observed changes in cytoarchitecture are likely to have adverse effects on normal cell migration and other behaviors associated with morphogenesis, resulting in abnormal outflow tract remodeling. These findings are consistent with functional studies of the role of Wnt11-R in *Xenopus laevis* heart morphogenesis[43]. Although Wnt11, TGFβ2 and the ATF2 family are required *in vivo* for cardiac morphogenesis, family redundancy in mouse embryos may obscure a requirement for this pathway in normal somite morphogenesis, as Wnt5A and Wnt11 are coexpressed in the dermomyotome (data not shown), like TGFβ2 and TGFβ3 (ref. 44). Wnt11 is required for normal somite morphogenesis in the chick, where Wnt5A is not coexpressed[16]. Our results also highlight a requirement for Wnt11 in the integration and crosstalk between three major signaling pathways—the canonical Wnt pathway, the

noncanonical Wnt pathway and TGFβ signaling—in achieving correct cardiac outflow tract morphogenesis.

METHODS

Mice

Pitx2$^{+/-}$ (refs. 45,46) and *Wnt11*$^{+/-}$ mice[19] have been described previously. Looptail mutant mice of the LPT/Le stock were obtained from The Jackson Laboratory. The ATF2 dominant-negative transgenic construct was created by inserting the *D. melanogaster* engrailed repression domain (amino acid residues 1–296) as an in-frame fusion to the mouse ATF2 DNA binding domain (residues 74–370) downstream of the CMV-chicken β-actin promoter. The transgenic reporter construct pTGFβ2 prom.LacZ was constructed by inserting 3.2 kb of *Tgfb2* promoter sequences and 1.2 kb of 5′ UTR sequences upstream of a lacZ reporter gene followed by 6.3 kb of intron 1 sequence. Plasmid pTGFβ2 prom.(mATF2): LacZ was constructed by mutating ATF2/CREB binding sites (GTCACT was changed to GGCCGC at −69 to −64, TGACGT was changed to CCGCGG at −1808 to −1803, TGACGA was changed to CCGCGG at −2952 to −2957; numbering refers to position upstream of the *Tgfb2* promoter that drives expression of *lacZ*).

Whole-mount RNA *in situ* hybridization and histological analyses

Whole-mount RNA *in situ* hybridization was carried out as previously described[47]. We used probes specific to the following genes (with the source of the sequence in parentheses; see below for GenBank accession numbers): *Wnt11* (sequence determined by A.M.), *Tgfb2* (GenBank EST); *Hspg2* (also known as *Perlecan*; GenBank EST); *Bmp4* (ref. 48); *Fgf8* (ref. 49); *Tbx1* (A. Baldini, Baylor College of Medicine); *Pitx2* (ref. 50); *Edn1* (GenBank EST); *Notch1* (GenBank EST). For histological analyses, mouse embryos were fixed in 4% paraformaldehyde, dehydrated and embedded in paraffin, cut into 8-μm-thick sections using a microtome and stained with hematoxylin-eosin according to standard protocol.

Immunofluorescence and immunohistochemistry

For immunofluorescence, mouse embryos were saturated with 20% sucrose and then frozen in OCT component and cut into 5-μm-thick sections on a cryostat. Sections were fixed in 2% paraformaldehyde for 10 min at 25 °C, blocked and stained with antibodies. Mouse embryos for immunohistochemistry were fixed in 4% paraformaldehyde, dehydrated and embedded in paraffin and cut into 5-μm-thick sections on a microtome. Phalloidin (#A-123790) was purchased from Molecular Probes. We used antibodies to the following proteins: laminin α-5 (see Acknowledgments); Scribble (provided by W.V.d.V.); MF20 (Developmental Studies Hybridoma Bank, University of Iowa); α-smooth muscle actin (clone 1A4, Sigma); VE-cadherin (#550548, BD Biosciences); PECAM-1 (#550247, BD Pharmingen); integrin-β1 (#Sc9970, Santa Cruz) and N-cadherin (#808-827, Calbiochem). Alexa Fluor 488 or 546 secondary antibodies were from Molecular Probes. Biotinylated secondary antibodies were from Vector Laboratories. Cell proliferation was detected using rabbit anti–phosphohistone H3 (#06-570, Upstate Biochem), and apoptosis was detected using rabbit anti–cleaved caspase-3 (#9661, Cell Signaling Technology).

RNA interference and RNA profiling

Plasmid-based RNA interference (shRNA) experiments were carried out as previously described using the pSUPER vector (T. Brummelkamp, The Netherlands Cancer Institute). The sequence used to design *Pitx2* siRNA is available as requested. A *Pitx2* siRNA expression vector was then cotransfected with a GFP expression vector at a ratio of 10:1 into C2C12 cells by Lipofectamine 2000 (Invitrogen). Two days later, GFP-positive cells were collected with a FACSCalibur cell sorter (BD Biosciences). Total RNA was extracted using an RNeasy Mini Kit (Qiagen). Genome-wide RNA profiling of C2C12 cells was performed on Codelink three-dimensional platforms (BioGem Core, University of California San Diego).

ChIP assays

For the ChIP assays, C2C12 cells were serum starved for 48 h, and control LacZ medium or Wnt11-conditioned medium or LiCl (10 mM) was added for 1 h before harvest. Cells were washed twice with PBS and cross linked with 1% formaldehyde for 10 min at 25 °C. For *in vivo* ChIP experiments, extracts were prepared from E8.75–E9.5 wild-type mouse hearts. Embryos were dissected in ice-cold PBS. After gentle pipetting, we cross-linked tissue with 2% formaldehyde for 2 h at room temperature. Cross-linked cells were then resuspended in 0.3 ml lysis buffer (1% SDS, 10 mM EDTA, 50 mM Tris-HCl pH 8.1 and protease inhibitors) and sonicated three times for 10 s followed by centrifugation for 10 min. Immunoprecipitation and washes were performed as described previously[10]. Precipitates were eluted three times with 1% SDS and 0.1 M $NaHCO_3$. Eluates were pooled and heated at 65 °C for 6 h to reverse the formaldehyde cross-linking. DNA fragments were purified with a QIAquick Spin Kit (Qiagen). For PCR, 1 μl of template from a 50-μl DNA extraction and 25 cycles of amplification were used with the appropriate promoter-specific primers. Sequences of the oligonucleotide primers are available in Supplementary Table 1 online. Antibodies used in ChIP experiments included anti-Pitx2 from guinea pig[10], anti-β-catenin (H-102) and anti-HDAC1 (H51) from Santa Cruz Biotechnology.

Real-time RT-PCR analyses

Real-time thermal cycling was performed using an Mx3000P thermal cycler (Stratagene) with SYBR Green Master Mix (Stratagene). Sequences of the oligonucleotide primers used for RT-PCR analysis are available in Supplementary Table 1.

Promoter cloning and luciferase transfection assay

A 2.0-kb genomic DNA fragment upstream of the *Wnt11* (ENSMUST 00000033005) start codon was amplified with a high-fidelity DNA polymerase (Novagen, 71086-3) and cloned into pGL3-basic vector (Promega, E1751). Sequences of primers used in the amplification of the *Wnt11* promoter are available in Supplementary Table 1. The QuikChange sited-directed mutagenesis kit (Stratagene, 200518) was used to make point mutations in Pitx2 binding sites (GAATCC→GCCGTT) in the promoter region according to the manufacturer's protocol. A genomic DNA fragment spanning bases −77 to +63 bp of *Tgfb2* (relative to the transcriptional start codon) was cloned into pGL3-basic vector. Sequences of primers used in the amplification of the *Tgfb2* promoter are available in Supplementary Table 1. A *Tgfb2*

promoter with an ATF2 binding site mutation was created by mutating CGTCAC to TGGCAC in the promoter region. Transfections were carried out in C2C12 cells according to standard techniques by Lipofectamine 2000 (Invitrogen). The cells were lysed 48 h after transfection, and luciferase and β-galactosidase activities were measured on a Luminoskan Ascent luminometer (Thermo Labsystems). For luciferase reporters, CMV-β-galactosidase was used to control for transfection efficiency. Normalized luciferase activities were compared with a pGL3 control to calculate the extent of repression. Data are presented as relative activity (compared with basal promoter activity) and are expressed as the mean ± s.d. of triplicates from a representative experiment. Each experiment was repeated three times. For siRNA transfection, control siRNA, *ATF2* siRNA, *Pitx2* siRNA and β-catenin siRNA were from Qiagen. The effects of these siRNAs on cellular protein expression are illustrated in Supplementary Figure 1 online.

X-gal staining of mouse embryos

Mouse embryos were fixed in 4% paraformaldehyde for 30 min on ice, permeabilized in PBS containing 0.02% nadeoxycholate and 0.01% NP-40 for 4 h at 25 °C and were then subjected to 5-bromo-4-chloro-3-indolyl-D-galactoside (X-gal) staining.

Cell culture and immunoblotting

Stably transfected Wnt11 and LacZ NIH3T3 cells were a gift (see Acknowledgments). To obtain Wnt11- and LacZ-conditioned media, we replaced the culture medium when cells had grown to 50% confluence and collected it 3 d later. The conditioned medium was centrifuged and stored at −20 °C. Wnt3A was purchased from R&D Systems. For JNK assays, cells were incubated in 0.5% serum 48 h before addition of Wnt-11- or LacZ-conditioned medium. When indicated, cells were pretreated for 2 h with SP600125 (AG Scientific) and treated with Wnt11-conditioned medium for an additional 1 h. Cells were lysed in 0.5% Nonidet P-40 lysis buffer. Samples were resolved on 12% SDS-PAGE and immunoblotted with anti-p-c-Jun, anti-p-ATF2, anti-β-catenin and anti-β-tubulin. Antibodies to phospho-ATF2, phospho-c-Jun and β-catenin were from Santa Cruz Biotechnology. Anti-β-tubulin antibody was from Sigma. Proteins were visualized by enhanced chemiluminescence detection (Amersham) using goat anti-mouse and anti-rabbit IgGs coupled to horse-radish peroxidase as the secondary antibody (Santa Cruz Biotechnology).

GenBank accession numbers

Tgfb2: BF135240; *Hspg2* (*Perlecan*): BQ713524; *Edn1*: AA511462; *Notch1*: BQ944558.

Supplementary Material

Refer to Web version on PubMed Central for supplementary material.

Acknowledgments

We thank A. Kispert (MH Hannover) for providing the Wnt11-transfected NIH3T3 cells, S. Ishii for providing the ATF2 mutant embryos and C. Marcelle for discussions and for sharing data before publication. We are grateful to J. Miner (Washington University) for providing us with the laminin α-5 antibody. We thank M. McCurdy, H. Taylor, L. Yang, L. Bu, X. Zhu, K.A. Ohgi, J. Zhao and C. Nelson for their technical assistance, J. Chen for helpful discussion and H. Taylor for animal husbandry. We also thank J. Hightower for figure preparation. M.G.R. is an

investigator with the Howard Hughes Medical Institute. This work was supported by US National Institutes of Health (NIH) grants HL74066, HL66276 and HL70867 (to S.M.E.); NIH grants HL65445 and DK18477 (to M.G.R.); NIH grant DK054364 (to A.P.M.); American Heart Association grant 0525141Y (to L.L.) and a Research Career Award from the US National Institute of Diabetes and Digestive and Kidney Diseases grant DK 064744 (to X.L.).

References

1. Veeman MT, Axelrod JD, Moon RT. A second canon. Functions and mechanisms of β-catenin-independent Wnt signaling. Dev Cell. 2003; 5:367–377. [PubMed: 12967557]
2. Henderson DJ, et al. Cardiovascular defects associated with abnormalities in midline development in the Loop-tail mouse mutant. Circ Res. 2001; 89:6–12. [PubMed: 11440971]
3. Phillips HM, Murdoch JN, Chaudhry B, Copp AJ, Henderson DJ. Vangl2 acts via RhoA signaling to regulate polarized cell movements during development of the proximal outflow tract. Circ Res. 2005; 96:292–299. [PubMed: 15637299]
4. Moon RT. Wnt/β-catenin pathway. Sci STKE. 2005; 2005:cm1. [PubMed: 15713948]
5. Chien KR. Myocyte survival pathways and cardiomyopathy: implications for trastuzumab cardiotoxicity. Semin Oncol. 2000; 27:9–14.
6. Srivastava D, Olson EN. A genetic blueprint for cardiac development. Nature. 2000; 407:221–226. [PubMed: 11001064]
7. Kelly RG, Buckingham ME. Modular regulation of the MLC1F/3F gene and striated muscle diversity. Microsc Res Tech. 2000; 50:510–521. [PubMed: 10998640]
8. Gruber PJ, Epstein JA. Development gone awry: congenital heart disease. Circ Res. 2004; 94:273–283. [PubMed: 14976138]
9. Alward WL. Axenfeld-Rieger syndrome in the age of molecular genetics. Am J Ophthalmol. 2000; 130:107–115. [PubMed: 11004268]
10. Kioussi C, et al. Identification of a Wnt/Dvl/β-Catenin→Pitx2 pathway mediating cell-type-specific proliferation during development. Cell. 2002; 111:673–685. [PubMed: 12464179]
11. Ganga M, et al. PITX2 isoform-specific regulation of atrial natriuretic factor expression: synergism and repression with Nkx2.5. J Biol Chem. 2003; 278:22437–22445. [PubMed: 12692125]
12. Campione M, et al. Pitx2 expression defines a left cardiac lineage of cells: evidence for atrial and ventricular molecular isomerism in the iv/iv mice. Dev Biol. 2001; 231:252–264. [PubMed: 11180966]
13. Christiansen JH, et al. Murine Wnt-11 and Wnt-12 have temporally and spatially restricted expression patterns during embryonic development. Mech Dev. 1995; 51:341–350. [PubMed: 7547479]
14. Kispert A, Vainio S, Shen L, Rowitch DH, McMahon AP. Proteoglycans are required for maintenance of Wnt-11 expression in the ureter tips. Development. 1996; 122:3627–3637. [PubMed: 8951078]
15. Lin L, et al. β-catenin directly regulates Islet1 expression in cardiovascular progenitors and is required for multiple aspects of cardiogenesis. Proc Natl Acad Sci USA. 2007; 104:9313–9318. [PubMed: 17519333]
16. Marcelle C, Stark MR, Bronner-Fraser M. Coordinate actions of BMPs, Wnts, Shh and noggin mediate patterning of the dorsal somite. Development. 1997; 124:3955–3963. [PubMed: 9374393]
17. Tanda N, Ohuchi H, Yoshioka H, Noji S, Nohno T. A chicken Wnt gene, Wnt-11, is involved in dermal development. Biochem Biophys Res Commun. 1995; 211:123–129. [PubMed: 7779076]
18. Schmidt M, Tanaka M, Munsterberg A. Expression of β-catenin in the developing chick myotome is regulated by myogenic signals. Development. 2000; 127:4105–4113. [PubMed: 10976043]
19. Majumdar A, Vainio S, Kispert A, McMahon J, McMahon AP. Wnt11 and Ret/Gdnf pathways cooperate in regulating ureteric branching during metanephric kidney development. Development. 2003; 130:3175–3185. [PubMed: 12783789]
20. Jiang X, Rowitch DH, Soriano P, McMahon AP, Sucov HM. Fate of the mammalian cardiac neural crest. Development. 2000; 127:1607–1616. [PubMed: 10725237]

21. Cai CL, et al. Isl1 identifies a cardiac progenitor population that proliferates prior to differentiation and contributes a majority of cells to the heart. Dev Cell. 2003; 5:877–889. [PubMed: 14667410]
22. Sanford LP, et al. TGFβ2 knockout mice have multiple developmental defects that are non-overlapping with other TGFβ knockout phenotypes. Development. 1997; 124:2659–2670. [PubMed: 9217007]
23. Bartram U, et al. Double-outlet right ventricle and overriding tricuspid valve reflect disturbances of looping, myocardialization, endocardial cushion differentiation, and apoptosis in TGFβ2-knockout mice. Circulation. 2001; 103:2745–2752. [PubMed: 11390347]
24. Torban E, Kor C, Gros P. Van Gogh-like2 (Strabismus) and its role in planar cell polarity and convergent extension in vertebrates. Trends Genet. 2004; 20:570–577. [PubMed: 15475117]
25. Costell M, et al. Hyperplastic conotruncal endocardial cushions and transposition of great arteries in perlecan-null mice. Circ Res. 2002; 91:158–164. [PubMed: 12142349]
26. Iozzo RV, et al. Structural and functional characterization of the human perlecan gene promoter. Transcriptional activation by transforming growth factor-beta via a nuclear factor 1-binding element. J Biol Chem. 1997; 272:5219–5228. [PubMed: 9030592]
27. Kispert A, Vainio S, McMahon AP. Wnt-4 is a mesenchymal signal for epithelial transformation of metanephric mesenchyme in the developing kidney. Development. 1998; 125:4225–4234. [PubMed: 9753677]
28. Bennett BL, et al. SP600125, an anthrapyrazolone inhibitor of Jun N-terminal kinase. Proc Natl Acad Sci USA. 2001; 98:13681–13686. [PubMed: 11717429]
29. Maye P, Zheng J, Li L, Wu D. Multiple mechanisms for Wnt11-mediated repression of the canonical Wnt signaling pathway. J Biol Chem. 2004; 279:24659–24665. [PubMed: 15067007]
30. Kim SJ, et al. Retinoblastoma gene product activates expression of the human TGF-β2 gene through transcription factor ATF-2. Nature. 1992; 358:331–334. [PubMed: 1641004]
31. Li H, Wicks WD. Retinoblastoma protein interacts with ATF2 and JNK/p38 in stimulating the transforming growth factor-beta2 promoter. Arch Biochem Biophys. 2001; 394:1–12. [PubMed: 11566021]
32. Ptashne M, Gann A. Transcriptional activation by recruitment. Nature. 1997; 386:569–577. [PubMed: 9121580]
33. Kawasaki H, et al. ATF-2 has intrinsic histone acetyltransferase activity which is modulated by phosphorylation. Nature. 2000; 405:195–200. [PubMed: 10821277]
34. Monzen K, et al. Smads, TAK1, and their common target ATF-2 play a critical role in cardiomyocyte differentiation. J Cell Biol. 2001; 153:687–698. [PubMed: 11352931]
35. Delot EC, Bahamonde ME, Zhao M, Lyons KM. BMP signaling is required for septation of the outflow tract of the mammalian heart. Development. 2003; 130:209–220. [PubMed: 12441304]
36. Yang L, et al. Isl1-Cre reveals a common Bmp pathway in heart and limb development. Development. 2006; 133:1575–1585. [PubMed: 16556916]
37. Reimold AM, et al. Chondrodysplasia and neurological abnormalities in ATF-2-deficient mice. Nature. 1996; 379:262–265. [PubMed: 8538792]
38. Maekawa T, et al. Mouse ATF-2 null mutants display features of a severe type of meconium aspiration syndrome. J Biol Chem. 1999; 274:17813–17819. [PubMed: 10364225]
39. Hummler E, et al. Targeted mutation of the CREB gene: compensation within the CREB/ATF family of transcription factors. Proc Natl Acad Sci USA. 1994; 91:5647–5651. [PubMed: 8202542]
40. Bleckmann SC, et al. Activating transcription factor 1 and CREB are important for cell survival during early mouse development. Mol Cell Biol. 2002; 22:1919–1925. [PubMed: 11865068]
41. van den Hoff MJ, Kruithof BP, Moorman AF. Making more heart muscle. Bioessays. 2004; 26:248–261. [PubMed: 14988926]
42. Murdoch JN, et al. Disruption of scribble (Scrb1) causes severe neural tube defects in the circletail mouse. Hum Mol Genet. 2003; 12:87–98. [PubMed: 12499390]
43. Garriock RJ, D'Agostino SL, Pilcher KC, Krieg PA. Wnt11-R, a protein closely related to mammalian Wnt11, is required for heart morphogenesis in *Xenopus*. Dev Biol. 2005; 279:179–192. [PubMed: 15708567]

44. Jakowlew SB, Ciment G, Tuan RS, Sporn MB, Roberts AB. Expression of transforming growth factor-beta 2 and beta 3 mRNAs and proteins in the developing chicken embryo. Differentiation. 1994; 55:105–118. [PubMed: 8143928]

45. Lin CR, et al. Pitx2 regulates lung asymmetry, cardiac positioning and pituitary and tooth morphogenesis. Nature. 1999; 401:279–282. [PubMed: 10499586]

46. Liu C, et al. Pitx2c patterns anterior myocardium and aortic arch vessels and is required for local cell movement into atrioventricular cushions. Development. 2002; 129:5081–5091. [PubMed: 12397115]

47. Wilkinson, DG., editor. In Situ Hybridization: A Practical Approach. Oxford Univ. Press; New York: 1992.

48. Lyons KM, Hogan BL, Robertson EJ. Colocalization of BMP7 and BMP2 RNAs suggests that these factors cooperatively mediate tissue interactions during murine development. Mech Dev. 1995; 50:71–83. [PubMed: 7605753]

49. Sun X, Meyers EN, Lewandoski M, Martin GR. Targeted disruption of Fgf8 causes failure of cell migration in the gastrulating mouse embryo. Genes Dev. 1999; 13:1834–1846. [PubMed: 10421635]

50. Campione M, et al. The homeobox gene Pitx2: mediator of asymmetric left-right signaling in vertebrate heart and gut looping. Development. 1999; 126:1225–1234. [PubMed: 10021341]

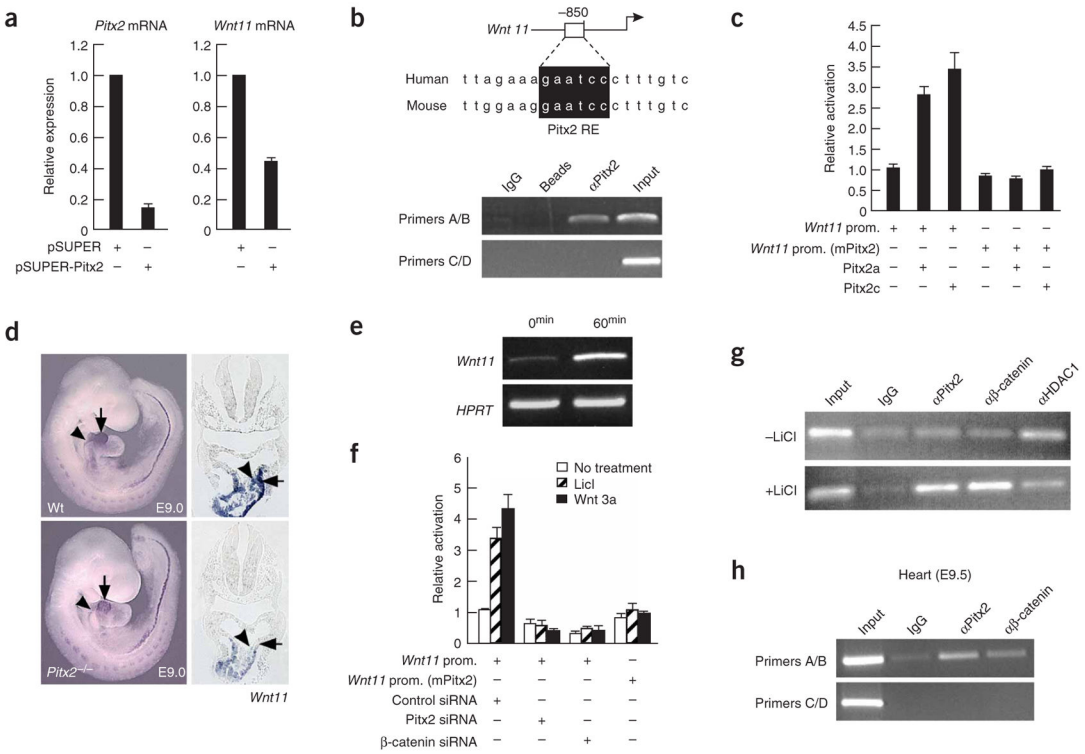

Figure 1.

Wnt11 is a downstream target of Pitx2 and β-catenin in muscle cell lineages and developing heart. (**a**) Real-time RT-PCR analysis of *Pitx2* and *Wnt11* transcripts in C2C12 cells transfected with pSUPER-Pitx2 or control vector (mean ± s.d. from three independent experiments). *Pitx2* and *Wnt11* levels were normalized to *Hprt1*. (**b**) Top: schematic of conserved Pitx2 binding site ~850 bp upstream of the transcription start site in the *Wnt11* promoter. RE, response element. Bottom: ChIP analysis using an anti-Pitx2 showed that Pitx2 was specifically recruited to the region containing the Pitx2 consensus site (primers A/B) but not to the 10-kb upstream region (primers C/D). (**c**) Reporter assay using a 2-kb *Wnt11* promoter-reporter with or without a Pitx2 binding site mutation in C2C12 cells. Cells were transfected with either Pitx2a or Pitx2c expression vector. Error bars represent s.d. (**d**) Whole-mount and section RNA *in situ* analysis of *Wnt11* expression in *Pitx2*-null embryos and wild-type littermates. (**e**) RT-PCR analysis of *Wnt11* expression in C2C12 cells after lithium treatment. (**f**) The *Wnt11* promoter was activated by canonical Wnt signaling dependent on Pitx2 binding. C2C12 cells were transfected with reporter and siRNAs as indicated and then treated with Wnt3A or LiCl before the luciferase reporter assay. Error bars represent s.d. (**g**) ChIP analysis of C2C12 cells in the absence or presence of both LiCl and serum using antibodies as indicated. (**h**) ChIP analysis of extracts from E9.5 embryonic heart. PCR was performed using primer pairs A/B and C/D.

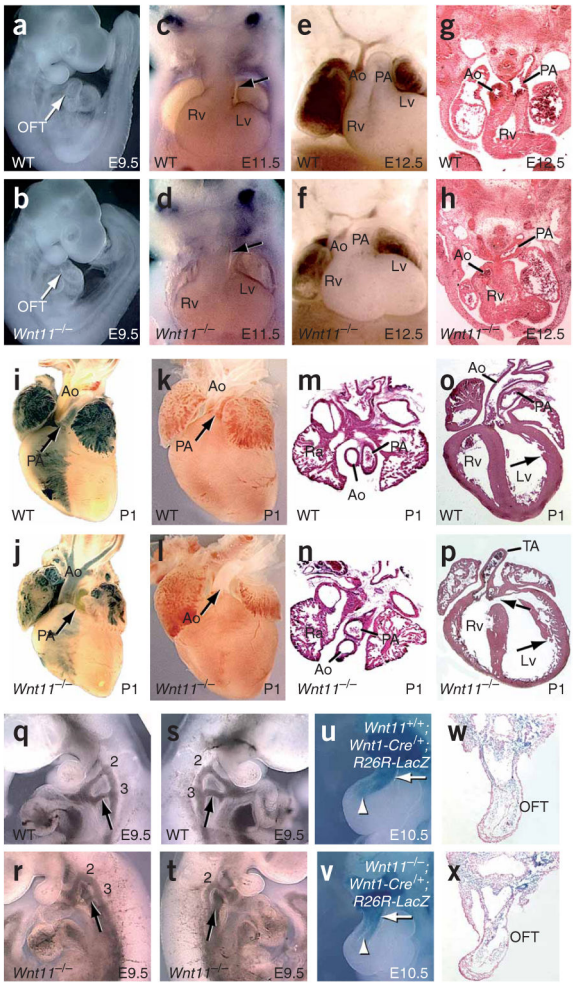

Figure 2.

Abnormal outflow tract and great vessel development in *Wnt11*$^{-/-}$ mutants. (**a**,**b**) Right lateral view of a wild-type embryo with normal outflow tract morphology (**a**, arrow) and a mutant with aberrant outflow tract (**b**, arrow) at E9.5. (**c**,**d**) Frontal view of a wild-type embryo with normal outflow tract morphology (**c**, arrow) and a mutant with aberrant outflow tract (**d**, arrow) at E11.5. (**e**,**f**) Frontal view of wild-type (**e**) and mutant (**f**) embryos at E12.5. Wild-type embryos show an aorta displaced dorsally and pulmonary artery displaced ventrally (to the front); in mutant embryos, relative placement of the great vessels is altered. (**g**,**h**) Transverse sections of embryos in **e** and **f**. (**i**,**j**) Frontal whole-mount view of postnatal day 1 (P1) wild-type (**i**) and mutant (**j**) hearts injected with plastic dyes. In wild-type hearts, liquid blue plastic injected into the right ventricle enters the PA (**i**), and yellow plastic injected into the left ventricle enters the aorta (**i**). In mutant hearts, blue plastic injected into the right ventricle enters the aorta, and subsequently the PA; yellow plastic injected into the left ventricle enters the PA (**j**), showing that the aorta is connected to the right ventricle and the PA is connected to the left ventricle in the Wnt11 mutant (*i.e.*, transposition of the great arteries (TGA, **j**), accompanied by a ventricular septal defect (VSD). (**k**,**l**) Whole-mount view of P1 wild-type (**k**) and another *Wnt11* mutant heart (**l**), with different configuration of

great vessels. (**m**,**n**) Transverse sections of wild-type (**m**) and mutant heart (**n**) show altered configuration of the great vessels: the aorta is connected to the right ventricle, and the PA is connected to the left ventricle in mutant hearts (**l**,**n**) (i.e., TGA). (**o**,**p**) Frontal sections of wild-type (**o**) and a different *Wnt11* mutant heart at P1. This mutant shows a single outflow tract vessel which is persistent truncus arteriosus (PTA) and also had a VSD (**p**, arrow), with a thin-walled ventricular myocardium (**p**, long small arrow). (**q**–**t**) Ink injection shows PAA defects in *Wnt11* mutants, with smaller left 3rd PAA (**r**, arrow) and no apparent right 3rd PAA (**t**, arrow) at E9.5. (**u**,**v**) Lineage tracing of neural crest cells by Wnt1-Cre; Rosa 26 R-floxed-*lacZ* in *Wnt11* mutant and wild-type background. (**w**,**x**) Transverse sections of embryos in **u** and **v**. OFT, outflow tract; PA, pulmonary artery; Ao, aorta; Rv, right ventricle; Lv, left ventricle; TA, truncus arteriosus; PAA, pharyngeal arch artery.

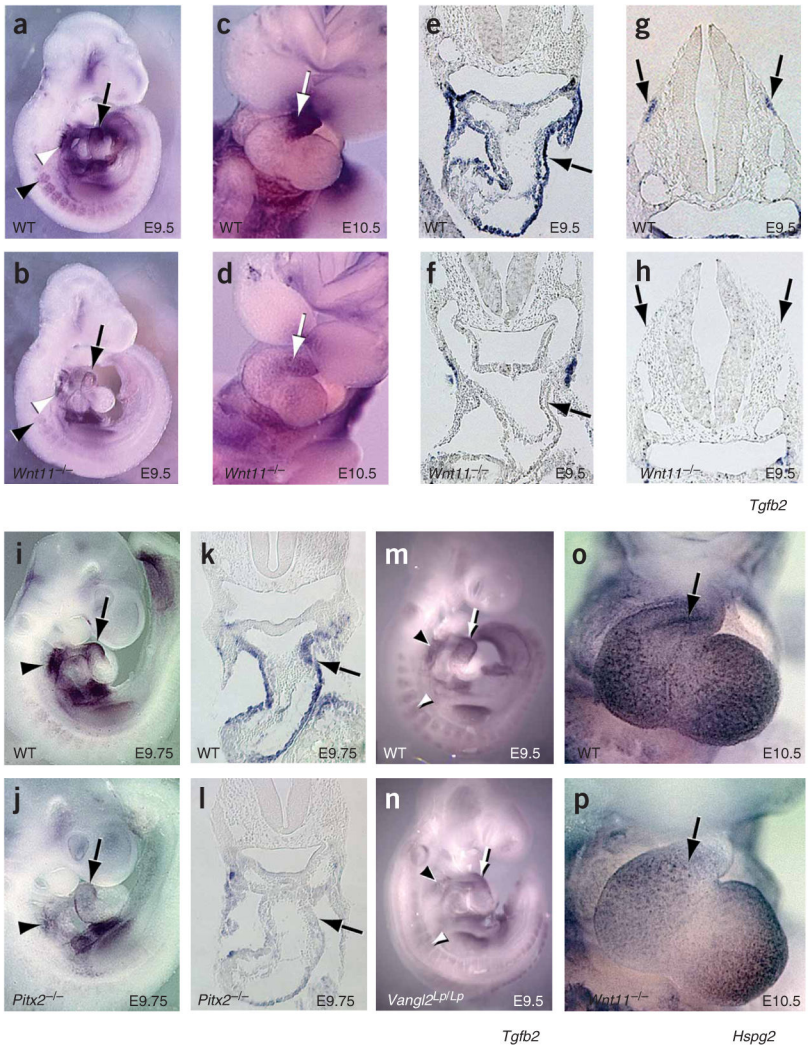

Figure 3.

Tgfb2 as a target of the Pitx2→Wnt11 signaling pathway. (**a**–**d**) Whole-mount RNA *in situ* hybridization with probes for *Tgfb2* in wild-type (WT) (**a**,**c**) and *Wnt11* mutants (**b**,**d**) at E9.5–E10.5. *Tgfb2* is downregulated in *Wnt11* mutants by E9.5 and at E10.5 in pharyngeal splanchnic mesoderm (white arrowhead), outflow tract (arrow) and somites (black arrowhead). (**e**,**f**) Section analysis of E9.5 embryos shows downregulation of *Tgfb2* mRNA in pharyngeal mesoderm, outflow tract myocardium and endocardium in *Wnt11* mutants (**f**) relative to wild-type littermates (**e**). (**g**,**h**) Section analysis of E9.5 embryos shows downregulation of *Tgfb2* mRNA in somitic mesoderm (arrow) in *Wnt11* mutants (**h**) relative to wild-type littermates (**g**). (**i**,**j**) Whole-mount RNA *in situ* hybridization with probes for *Tgfb2* in wild-type (**i**) and *Pitx2* mutants (**j**) at E9.75. *Tgfb2* expression is decreased in pharyngeal splanchnic mesoderm (arrowhead) and outflow tract (arrow) of *Pitx2* mutant embryos relative to controls. Section analysis (**k**,**l**) shows downregulation of *Tgfb2* in pharyngeal mesoderm, outflow tract myocardium and endocardium of *Pitx2* mutants. (**m**,**n**) Whole-mount RNA *in situ* hybridization with probes for *Tgfb2* in wild-type embryos (**m**) and *Vangl2* mutants (**n**). *Vangl2* mutants show down-regulation of *Tgfb2* in pharyngeal

splanchnic mesoderm (black arrowhead), outflow tract (arrow) and somites (white arrowhead) (**o**,**p**). Whole-mount RNA *in situ* with probes for *Hspg2* at E10.5. Outflow tract expression of *Hspg2* is severely downregulated in *Wnt11* mutants (**p**) relative to control littermates (**o**).

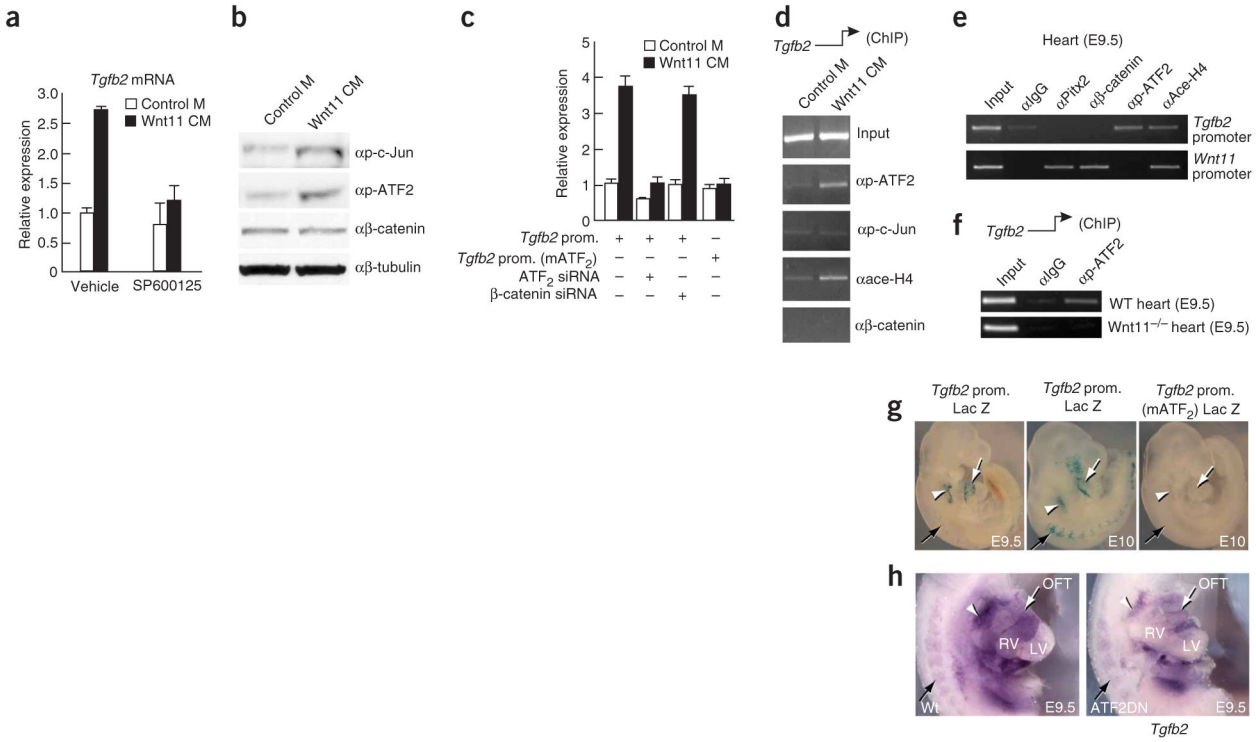

Figure 4.

Tgfb2 is regulated by a Wnt11→JNK→ATF/CREB pathway. (**a**) Real-time RT-PCR analysis of *Tgfb2* mRNA in C2C12 cells treated with Wnt11-conditioned medium (CM). *Tgfb2* mRNA expression is induced by 60 min of treatment with Wnt11 CM; this induction is inhibited by treatment with SP600125, a JNK inhibitor. *Tgfb2* levels were normalized to *Hprt1*; data represent mean ± s.d. from three independent experiments. (**b**) Protein blot of extracts from C2C12 cells treated with control medium (M) or Wnt11 CM. β-tubulin was a loading control. (**c**) Wnt11 activation of the *Tgfb2* promoter depends on ATF2. C2C12 cells were transfected with a *Tgfb2* promoter- reporter with or without an ATF2 binding site mutation and siRNA directed against either ATF2 or β-catenin. Cells were then treated with control medium (M) or Wnt11 CM before the luciferase assay. Error bars represent s.d. (**d**) ChIP analysis of C2C12 cells treated with control medium or Wnt11 CM using antibodies as indicated. (**e**) ChIP analysis of E9.5 heart extracts using antibodies as indicated. (**f**) ChIP analysis of E9.5 heart extracts from either control wild-type littermates or *Wnt11* mutant embryos. (**g**) Expression of the *Tgfb2* prom.LacZ or *Tgfb2* prom.(mATF2).LacZ constructs in transgenic mouse embryos. LacZ is expressed in pharyngeal splanchnic mesoderm (arrowheads), outflow tract (white arrows) and somites (black arrows). (**h**) Whole-mount RNA *in situ* hybridization with probes for *Tgfb2* in wild-type and dominant-negative ATF2 transgenic embryos. *Tgfb2* expression is decreased in pharyngeal splanchnic mesoderm (arrowheads), outflow tract (white arrows) and somites (black arrows) in dominant-negative ATF2 transgenic embryos. Ace, acetylated.

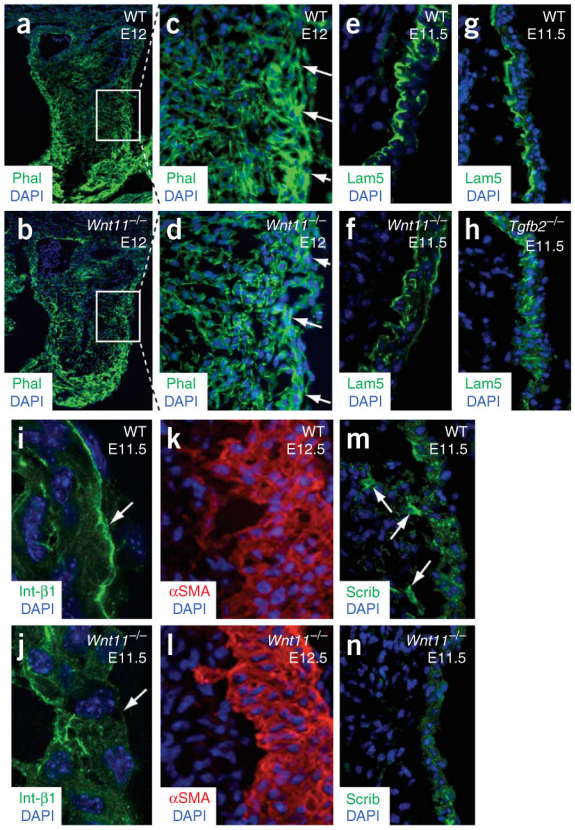

Figure 5.

Immunofluorescence analysis of sections from wild-type and *Wnt11* and *Tgfb2* mutant embryos. Sections were labeled with antibodies as indicated. Anti-laminin α-5 (Lam5), anti-Scribble (Scrib), anti-integrin-β1 (Int-β1) and anti-α-smooth muscle actin (αSMA) were used. (**a**–**d**) Phalloidin staining demonstrated a decrease in cytoskeletal actin in myocardial wall of the outflow tract in *Wnt11* mutants. **c** and **d** show higher-magnification views of outlined areas in **a** and **b**. In **e**–**n**, views shown are the left wall of the upper outflow tract (part of the inner curvature). (**e**–**h**) Laminin α-5 shows strong and asymmetric expression at the interface between the myocardium and mesenchyme of the wild-type outflow tract (**e**,**g**). In both *Wnt11* and *Tgfb2* mutants, the strength of laminin α-5 expression and its ordered asymmetrical distribution are reduced (**f**,**h**). (**i**,**j**) Immunostaining for integrin β1, a marker of basal lamina, demonstrated a clear basal lamina structure in the myocardial epithelium of the wild-type outflow tract (**i**). In contrast, integrin β1 appeared to be severely diminished or absent in Wnt11 mutants (**j**), suggesting a disruption of basal structures. (**k**,**l**) Staining with antibody to αSMA demonstrated the loose mesenchymal appearance of myocardial cells extending filopodia toward the cushion mesenchyme of the wild-type outflow tract at E12.5 (**k**). In contrast, in *Wnt11* mutants demonstrated a more compact, tightly adhering group of myocardial cells, with few filopodia (**l**). (**m**,**n**) Scribble protein showed a punctuate perimembranous distribution in wild-type outflow tract myocardium at E11.5, with scattered cells within the cushion mesenchyme expressing very high levels of Scribble (**m**). In *Wnt11*

mutants, there was a severe reduction in Scribble expression within the outflow tract myocardium, and no expression was observed within cushion mesenchyme cells (**n**).

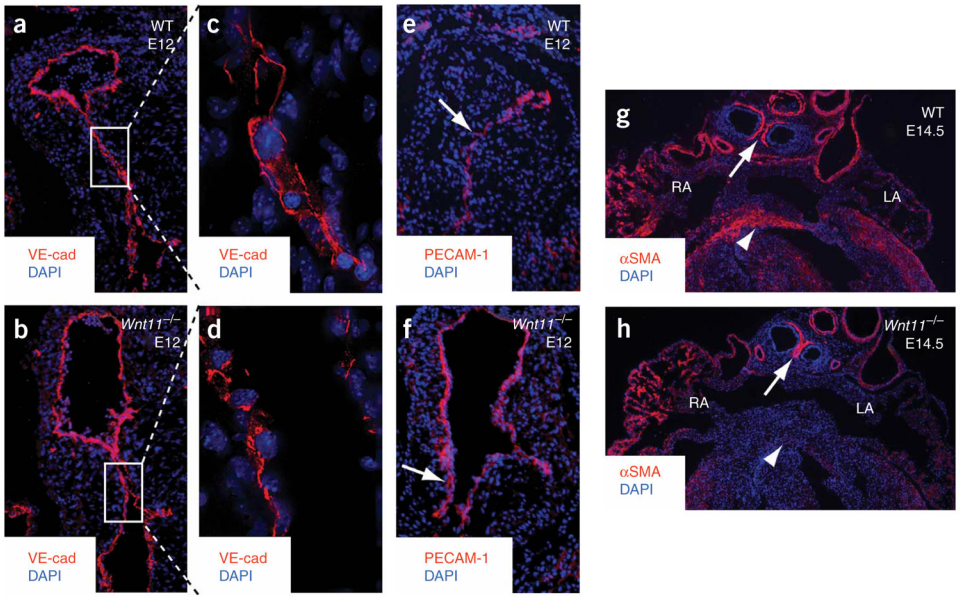

Figure 6.

Immunofluorescence analysis of endothelial cells from wild-type and *Wnt11* mutant embryos. (**a**–**f**) Immunostaining of endocardial cells using VE-cadherin and PECAM-1 antibodies. Note close apposition of two endothelial layers lining the outflow tract in wild-type embryos at E12 (**a**,**e**). In *Wnt11* mutants, in contrast, the two endocardial layers were not closely apposed (**b**,**f**). (**c**,**d**) Higher-magnification views of outlined areas in **a** and **b**. (**g**,**h**) Frontal sections of E14.5 wild-type and *Wnt11* mutant hearts immunostaining with anti-αSMA. αSMA is expressed in the proximal part of the outflow tract cushions, where they converge with the ventricular septum (**g**, arrowhead), as part of the process of myocardialization. No smooth muscle actin staining is observed in this region in *Wnt11* mutants (**h**, arrowhead). Smooth muscle actin is expressed by cardiac neural crest cells that surround the great vessels in wild-type embryos (**g**, arrow), and this expression is also observed in *Wnt11* mutants (**h**, arrow), suggesting that cardiac neural crest migration and differentiation have occurred appropriately.